

Design of carrot washing and grading machine

Mustefa Jarso^{1*}, Amana Wako²

(1. Department of Agricultural Engineering, Haramaya Institute of Technology, Haramaya University, Dire Dawa, 138, Ethiopia;

2. Department of Mechanical Engineering, Adama Science and Technology University, Adama, 1888, Ethiopia)

Abstract: Carrot washing and grading is performed after harvesting and before transporting to the market has been done with traditional methods by farmers in Ethiopia with too tedious, much time, and labor-consuming which leads to health problems, Fertile soil erosion, discouraging for carrot production and river water pollution. The main objective of this study was to design, develop, and perform the evaluation of carrot washing and grading machine after harvesting before transporting to market that was not used for cooking purposes to alleviate the above-stated problems. During design, a power source, initial speed, and discharge capacity of the pump were considered as 50 W, 6.28 m s⁻¹ and 0.036 L s⁻¹ respectively based on literature reviews. Performance of this machine evaluation was carried out with Nantey variety at two levels of feeding loads 10kg and 15 kg at different drum speeds; 1.47 m s⁻¹, 2.20 m s⁻¹, and 2.93 m s⁻¹. The data was collected in both qualitative and quantitative methods. The overall mean results obtained for performance indicators in terms of time required to complete washing and grading activities, washing efficiency, grading efficiency, percentage of damage root, and throughout put capacity were recorded as 2.22 minutes, 98.70%, 92.23%, 1.21%, and 242.17 kg h⁻¹, respectively. The results indicated that the time required of 2 to 10.88minutes, washing efficiencies of 84.87% to 98.70% or the range of the variable of drum speed between 1.47 to 2.93 m s⁻¹ and for the range of the variable of feeding load 10-15 kg. As the speed climbed from 1.47 to 2.93 m s⁻¹ and the feeding load rose from 10 to 15 kg, the grading efficiency increased from 72.89% to 92.23%. Each one of these machines cost \$313.18. The grading unit should be adjusted to a vibration mechanism by separating it from the washing unit in a layer of the machine frame because the carrot roots have low sphericity (30%), which led to some amounts of carrot roots being erroneously graded. Additionally, it is suggested that the pedal-turning mechanism be modified to serve the dual function of generating power that may be stored during operation and used at night in order to enhance rural electrification.

Keywords: carrot, washer, grading, pedal-operated, human power, pump

Citation: Jarso, M., and A. Wako. 2023. Design of carrot washing and grading machine. *Agricultural Engineering International: CIGR Journal*, 25(1): 225-249.

1 Introduction

The carrot is one of the most important and healthy vegetables for people since it contains healthy components (Jahanbakhshi et al., 2018; Surbhi et al., 2018; Ahmad et al., 2019; Bhattarai et al., 2017; Bender et al., 2020). The

carrot is grown in many different countries, including Ethiopia, because of its nutritional advantages and other applications (Bhattarai et al., 2017; Yadav, 2020; CSA, 2020). In Ethiopia, carrots are mostly grown in Oromia, Amhara, Addis Abeba, Tigray, and SNNPR at elevations of 300 to 3000 masl (CSA, 2020). Ethiopia has the lowest annual production among developing countries even if it can produce in a variety of agro-ecologies (FAO, 2018). As a result, there are less carrots available, which contributes to various ailments like vitamin A insufficiency (Tabor and Yesuf, 2012). These show that a key factor in

Received date: 2022-03-15 **Accepted date:** 2022-07-11

***Corresponding author: Mustefa Jarso,** Lecturer, Department of Agricultural Engineering, Haramaya Institute of Technology, Haramaya University, Dire Dawa, 138 Ethiopia. Tel: +251-921-93-3069. Email: musxee@gmail.com.

reducing the aforementioned and other ailments in Ethiopia is the production and promotion of carrots for consumption.

Post-harvest procedures like washing and grading carrot roots are carried out after harvest and before they are delivered to markets in order to enhance product quality and market appeal, decrease post-harvest loss, remove soil and debris, lower product temperature, and minimize microbial load (Alam et al., 2018). These post-harvest actions have also a considerable impact on the production and consumption of carrots. Farmers do not properly cultivate the carrots when these tasks are not mechanized because they are worried about the tedious tasks that will come their way in the future. In addition, because of the tedious tasks such as washing and grading that will befall them in the following phase, the farmed crop is not properly gathered. These and comparable circumstances make farmers immoral for growing carrots if the subsequent processes are not effectively mechanized. Ethiopians have done it entirely using conventional ways. Women and children, in particular, are the primary participants in the activities.

Traditionally they frequently wash carrot roots by hand or feet in rivers or ponds, then grade them by hand into the desired size which is too time-consuming and labor-intensive, resulting in health problems and large post-harvest losses (Bhattarai et al., 2017). According to a non-structured discussion with farmers and a tour of the field, traditional washing involves more laborers or employees, more time, and exposes them to various health problems as a result of the extended duration of work.

To overcome the drudgery and negative effect of the traditional method, different carrot and fruit washing machines operated by electric motors, engines, and manually cranked by hands were designed and developed in different countries with 1.10-2.93m/s of drum recommended to wash the carrot roots sample about 10-15kg (Anjali and Ikhar, 2018). Using Electric motor machines in a rural area is difficult due to the scarcity of electric power distribution. The engine-operated machines

are energy-intensive and expensive which need considerable initial capital investment that is not appropriate for small-scale farmers. According to Seweh et al. (2016), quickly and easily installing electric motor and engine machines is difficult in rural areas. The manually operated or hand-cranked machines are one of the options for rural areas, however, due to it needing huge human energy to crank, it must be replaced with other appropriate methods such as pedal operating machines because anyone can generate using leg pedaling about 2-4 times power of hand crank or 50-150 W at 5.24-10.47 m s⁻¹ under different conditions and loads (Mushiri et al., 2017; ; Krishnamurthy et al., 2017) .

Even if manual, electric motor, and diesel carrot washing machines were conceived and produced around the world, none of them were adopted and delivered to Ethiopia. Furthermore, no grader was created to assist farmers in grading carrots according to market criteria. As a result, the carrot is Ethiopia's forgotten crop that has yet to be mechanized. Because it is washed and graded by boring mechanisms, its post-harvesting is quite high and its quality is very low.

Finally, carrot roots should be washed and graded to raise the product's quality and marketability. In order to reduce laboriousness and motivate farmers to cultivate carrots, these tasks should be mechanized. The developed and constructed washing machines with various power sources that are suitable for small-scale farmers have not been adopted or used in Ethiopia. Additionally, no technology exists to assist farmers in grading carrots per their needs. The main objective of this project is to design and develop a pedal-operated machine that is straightforward, affordable, and energy-efficient using components from the local market.

2 Materials and methods

2.1 Determination of physical properties of carrot roots

100 freshly harvested samples of carrots from local varieties grown in the Arsi Zone, Shirka District, which is located at latitude and longitude of 07°37'N 39°30'E and

has an elevation of 2353 meters above sea level, were chosen at random for the purpose of measuring various physical attributes. Since the country's primary area for producing carrots is this location (Tabor and Yesuf, 2012).

2.1.1 Dimension of carrot roots

The major diameter, intermediate diameter, and minor diameter were measured using a vernier caliper of a with an accuracy of 0.05 mm and a measuring range of 0.00 – 150.00 mm using a procedure developed by Gautam et al. (2016).

2.1.2 Geometric mean diameter and sphericity

Geometric mean diameter and sphericity were determined after the the major, intermediate, and minor diameters were measured by using Equations 1-2 (Jahanbakhshi et al., 2018) which are used to. fix the gap between slots and slots shape, respectively.

$$D_g = \sqrt[3]{abc} \quad (1)$$

$$\phi = \frac{D_g}{a} \quad (2)$$

where, a is the major diameter (mm), b is the intermediate diameter (mm), c is the minor diameter (mm), D_g is the geometric mean diameter and (mm) and ϕ is the sphericity (%).

2.1.3 Bulk density

The bulk density of carrot roots were determined from box having 200 mm, 152 mm, and 71 mm length, width, and height respectively with the sample mass 1375g after harvesting from three different fields and the average bulk density was taken using Equation 3 to determine the volume of the drum (Bashar et al., 2014; Soyoye et al., 2018).

$$\rho_b = \frac{m}{V} \quad (3)$$

where, ρ_b is the bulk density of the sample (g cm^{-3}), m is the mass of sample (g), and V is the volume of the sample (cm^3).

2.1.4 Coefficient of friction

Static coefficient determined by the inclined plane method using wood surfaces. Timber raised from the bench table with an angle of θ . Then by solving the free body

diagram of static

conditions, the static friction coefficient can be determined by Equation 4 in order to determine length of inlet and outlet ports for easily unloading the washed roots (Jahanbakhshi et al., 2018).

$$\mu_s = \frac{\sin \theta}{\cos \theta} \quad (4)$$

where, μ_s is the static coefficient of friction.

Similarly, taking into consideration the kinetic conditions and uniform acceleration equations, the kinetic friction coefficient calculated by Equation 5 and is always smaller than the static friction coefficient (Bayram et al., 2019; Boukouvalas et al., 2010; Jahanbakhshi et al., 2018).

$$\mu_k = \frac{g \sin \theta - a_x}{g \cos \theta}, a_x = \frac{2d}{\Delta t^2} \quad (5)$$

where, μ_k is the kinetic or dynamic coefficient of friction, d is the sliding distance of the timber (m), Δt^2 is the time(s) for the object to slide along the distanced, g is acceleration due to gravity and a_x is the uniform acceleration of the object (m s^{-1}).

2.1.5 Angle of repose

The angle of repose for carrot root was determined to reduce the damage occurred between roots themself. It determined with a bottomless box. The box was placed on a horizontal surface and filled with a sample then gradually lifted. Allowing the sample to accumulate and form a conical heap on the surface. The diameter of the conical shape formed by the carrots sample (D) and two opposite sides (L_1 and L_2) were measured with rulers and the angle of repose (ϕ) was estimated using Equation 6) (Teferra, 2019).

$$\phi = \cos^{-1} \left(\frac{D}{L_1 + L_2} \right) \quad (6)$$

2.2 Description of pedal operated carrot washing and grading machine

The pedal-operated carrot washing and grading machine consist mainly of four parts: the pedal assembly (power transmission unit), the reciprocating pump assembly, washing and grading cylinder, and supporting frame as shown in Figure 1.



Figure 1 Manufactured carrot washing and grading machine

Operator seat, pedal, chain, shafts, sprocket, pulleys and belts, and crank make up the pedal assembly. The pedal rotates the chain, which is connected to the sprocket, and the transmission shaft, which is connected to the horizontal frame, at a 60° angle. The idler shaft with idler shaft pulley and the power transmission shaft with transmission shaft pulley were installed on the vertical frame at a 30° angle. To reciprocate connecting and piston rod for pump operation, the crank is welded to the transmission shaft on the other side. The idler pulley shaft is vertically aligned with the washing and grading cylinder shaft, which is located on the top of the frame. The water pump, suction, and delivery pipelines make up the reciprocating pump assembly. The pump creates a vacuum and pulls water from the source to the washing and grading drum through the perforated drum hollow shaft as the crank reciprocates connecting and piston rods.

Washing and grading units make up the washing and grading cylinder drum. The washing machine is of the cylindrical form, with eighteen pcs of rectangular wood boards that were calculated. According to Ambrose and Annamalai (2013), these timbers should be separated by 2

mm to allow only water and contaminants to flow through. To receive the most washing time, this unit was 70 cm length. A trapezoidal timber enlargement of the washing unit makes up the grading unit. The geometric mean diameter of carrots was used to make these trapezoidal timbers, which are 2 mm at the start and 30 mm at the end. This enables gardeners to obtain carrot tubers that are roughly sorted in order of size. As a consequence, the grading unit primarily performs two grading based on the size used for local and international markets. This unit was limited to an 80 cm length, which was determined by trial and error.

The washing and grading drum is kept at an angle to allow the product to move easily to the outlet port without stopping the activities based on the calculated coefficient of Friction carrot roots. The unwashed and ungraded carrots are entered into the unit by opening the door hinged on the washing parts.

2.3 Machine operation

The operation began with rotating the pedal that rotates the transmission shaft through the sprocket and chain. The motion of the transmission shaft transmits to the Idler shaft

and cranks simultaneously. The Idler shaft is used to reduce the speed of the transmission shaft with 4:1 ratios and rotate the washing and grading unit through the belt and pulleys. Carrot roots were fed into the inclined and rotating cylinder from the inlet door and traveled down along the length of the cylinder. Carrot roots at the lower portion of the cylinder were lifted upwards by the trapezoidal slot, from which they are again lifted along with it and slid down. They gradually move toward the opposite end of the cylinder from the inlet port and are forced to pass through the slots during the rotation of the cylinder based on their diameters.

The crank transfers the transmission shaft motion to the connecting rod. The connecting rod converts the rotational motion of the crank to reciprocating motion and transfers it to the piston rod. The piston with rubber piston rings is connected to the piston rod. These parts reciprocate through the cylinder and create the vacuum to suck water from the river or any water storage and deliver to the washing and grading unit through the delivery pipe and perforated hollow shaft for washing. In addition to the pedal, a handle was added that could perform every activity mentioned above in case of pedal or chain failed.

2.4 Design considerations and assumptions made

Before starting the design and construction of the Carrot washer and grader, the following factors were considered for the appropriate selection of materials, to obtain high efficiency, to obtain reduced cost and post-harvest losses, and to add the product quality.

to extend the life of the machine, relatively waterproof wood was taken into consideration when choosing materials for the drum design.

Considering corrosion, the machine's metal components were coated.

To lower the cost of the machine, all of its components were manufactured using materials that could be found nearby.

To make the machine adaptable, simple to assemble, and maintained, the majority of its components were connected to one another using bolts and nuts. Machine

size, loading and unloading, and easily operable by village artisans were taken under consideration for flexibility and portability.

To introduce the appropriate amount of water into the drum for washing, the compatibility of the water pressure that pushes water from the pump to the washing and grading drum and the flow rate into the drum were taken into consideration

Assumptions Made

During the design of the carrot washing and grading machine, the following assumptions were made based on the literature reviews.

For making machines easily operating by all categories of human ages, 50 watts power selected as input power (Mushiri et al., 2017; Ajay et al., 2014).

Since most people pedal efficiently and continuously for an hour or more in the range of 5.24 to 7.33 m s⁻¹; for simplicity's sake, 6.28 m s⁻¹ is used as pedal speed during calculation (Bhatawadekar et al., 2015).

11 to 15 L of water is recommended to wash 7 to 20 kg carrot sample in 5 to 7 minutes, so the average discharge rate for washing was assumed to be 0.036 l s⁻¹ (Ambrose and Annamalai, 2013; Moos et al., 2002).

1.05- 2.93 m s⁻¹ of drum recommended to wash the carrots roots sample about 10 kg-15 kg, therefore, 2.93 m s⁻¹ and 10 kg were considered for the design calculation of this machine (Ambrose and Annamalai, 2013; Moos et al., 2002).

2.5 Selection of power transmission components

The bicycle chain wheel having a diameter of 150 mm and 36 teeth, the sprocket 85 diameter with teeth number 20, and the pedal having a diameter of 320 mm were selected and bought arbitrarily from the market. The speed of the smaller sprocket (111.31 m s⁻¹) was determined by Equation 7 from the relation of the number of teeth on the chain wheel and sprocket because the power transmitted by a chain from wheel shaft to sprocket shaft is equal to input power (Adegbite et al., 2019).

$$N_{sprocket} = \frac{N_{wheel}T_{wheel}}{T_{sprocket}} \quad (7)$$

Where, $N_{sprocket}$ =speed of sprocket ($m s^{-1}$), N_{wheel} =speed of chain wheel ($m s^{-1}$), T_{wheel} =teeth numbers on the chain wheel, and $T_{sprocket}$ =teeth numbers on the sprocket

Based on the chain selection procedures cross ponding with smaller sprocket speed which was $11.31 m s^{-1}$, the chain which has 90 cm and standardized by chain designation 06B were selected.

The drum speed was assumed as $2.93 m s^{-1}$ for the design calculation of this machine and the speed of the smaller sprocket was calculated as $11.31 m s^{-1}$. Therefore, power from the transmission shaft pulley is delivered to the drum shaft pulley with a speed reduction ratio of 4:1. To achieve this ratio, the minimum pulley size for “A” type V-belt 75 mm was selected for driver pulleys on the crankshaft and idler shaft. The driven idler pulley was also arbitrarily determined to 140 mm by considering the output speed. Based on the crank (transmission) shaft pulley speed, drum shaft pulley speed, the diameter of driver pulleys, and the diameter of idler driven pulley, the diameter of drum shaft pulley estimated as 155 mm using Equation 8 (Adekanye et al., 2016).

$$\frac{N_4}{N_1} = \frac{D_1 \times D_3}{D_2 \times D_4} \quad (8)$$

where, N_1 is the angular speed of the first driver in rpm on the first belt, N_4 is the angular speed of the last in rpm on the second belt, D_1 is the diameter of the first driver (mm), D_2 is the diameter of the first follower (mm), D_3 is the diameter of the last driver (mm), and D_4 is the diameter of the last follower (mm).

The selection of belt was made by using the nominal pitch lengths ($L_1 = 708.51mm$) and ($L_2 = 735.93mm$) and center distances ($x_1 = 185.5mm$) and ($x_2 = 187.5mm$) from transmission shaft pulley to idler shaft pulley and from idler shaft pulley to drum shaft pulley that determined by Equations 9 and 10 respectively (Umani and Markson, 2020).

$$x = \frac{D_1 + D_2}{2} + D_2 \quad (9)$$

$$L = \frac{\pi}{2}(D_1 + D_2) + 2x \quad (10)$$

where, D_1 is the diameter of the larger pulley (mm), D_2

is the diameter of the smaller pulley (mm), and x is the distance between the centers of two pulleys (mm).

The nearest standard pitch lengths for calculated L_1 and L_2 are 710 mm and 730 mm respectively. So based on minimum pulley diameters (75 mm) recommended for standard V-belts, the nearest standard pitch lengths, and minimum center distance; the belt sizes of A-28 and A-29 were sufficient to transmit power from the transmission shaft to idler shaft and from the idler shaft to washing and grading cylinder.

2.6 Developing and design of pump assemblies

Tap water is not common in rural areas; therefore, the thrown hydraulic cylinder not used again for vehicles maintained and adjusted for carrot washing machine as reciprocating pump which drive by pedal and used to suck water from river or any kind of reservoir and send to washing drum. This developed and selected pump has 75 mm, 25 mm, and 14 mm cylinder length, bore, and rod diameter respectively.

2.7 Connecting rod design

The maximum fluid pressure (p) and the maximum force (F_L) on the piston due to pressure is calculated as Equations 11 and 12 respectively (Goud and Sumalatha 2018; Shankar et al., 2016; Thorat and Patil, 2015; Ashiedu et al., 2016).

$$P_{th} = p \quad (11)$$

$$F_L = Ap \quad (12)$$

where, P_{th} is the theoretical power required to drive the pump (50 W), F_L is the the maximum force on the piston due to pressure (500 N), p is the maximum pressure of the fluid (0.001 MPa), and A is the cross-section area of the piston (0.0005 m²).

The connecting rod is subjected to an axially compressive force which is equal to maximum fluid force (F_L), it is designed as a strut or column (Antony et al., 2016). The buckling loads about X-axis (W_{cr} about x-axis) and about Y-axis (W_{cr} about y-axis) is calculated according to Rankine’s formula as given by Equations 13 and 14 respectively. (Bharath Kumar et al. 2015; Mukkawar et al., 2015; Nitturkar et al., 2020).

$$W_{cr} \text{ about } X - \text{axis} = \frac{\sigma_c A}{1 + a \left(\frac{l}{k_{xx}} \right)^2}, \text{ for both end hinge}$$

$$L = l \tag{13}$$

$$W_{cr} \text{ about } Y - \text{axis} = \frac{\sigma_c A}{1 + a \left(\frac{l}{k_{yy}} \right)^2}, \text{ for both end fixed}$$

$$L = \frac{l}{2} \tag{14}$$

where, A is the cross-sectional area of the connecting

rod, l is the length of the connecting rod, σ_c is the compressive yield stress, σ_c is 330 Mpa for steel, W_{cr} is the crippling or buckling load, I_{xx} and I_{yy} are moment of inertia of the section about X-axis and Y-axis respectively, k_{xx} , and k_{yy} are the radius of gyration of the section about X-axis and Y-axis respectively, a is a constant, 1.33×10^{-4} for mild steel.

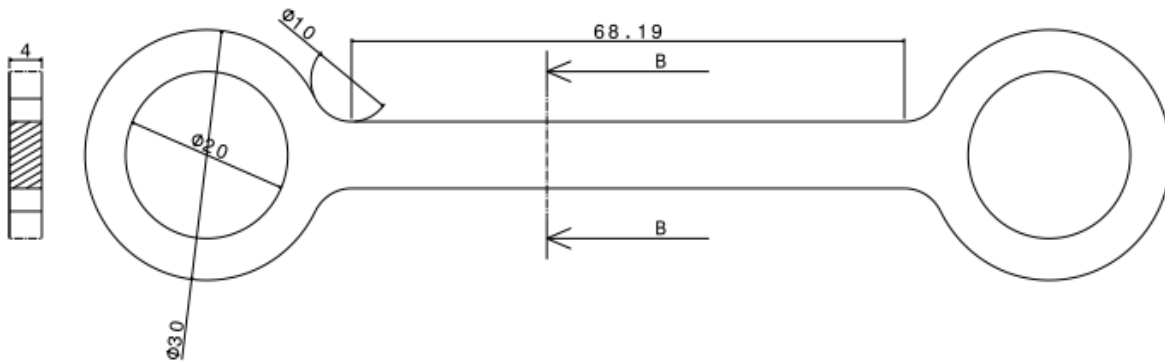


Figure 2 Connecting rod section view (all dimensions are in mm)

Because there is clearance on both sides of the cylinder, the cylinder's length is 15 percent greater than the stroke's length. As a result, the length of the stroke (s) was calculated as $s=75 \text{ mm}/1.5=50 \text{ mm}$. The radius of the crank (r) is also half of the stroke length ($r=1/2=25 \text{ mm}$), and the length of the connecting rod (l) is equal to the stroke length (75 mm) (Bharath Kumar et al., 2015). Since the connecting rod is designed by taking the force in the connecting rod (F_C) equal to the maximum force on the piston due to water pressure (F_L), therefore force in the connecting rod, $F_L=F_C=500 \text{ N}$

The connecting rod is designed for buckling about the X-axis (i.e. in a plane of motion of the connecting rod), assuming both ends are hinged then the buckling load is determined as given by Equation 15 (Vegi and Vegi, 2013).

$$W_{cr} = F_C \times F.O.S. \tag{15}$$

where, $F.O.S.$ is the factor of safety. Let's consider $F.O.S.$ as 10, then $W_{cr} = 1759.29 \text{ N} \times 10 = 5000 \text{ N}$.

To have a connecting rod equally strong in buckling about both the axes, the buckling loads must be equal and make the Equations 13 and 14 equal, then the connecting rod is four times strong in buckling about Y-axis than about X-axis as mentioned by Equation 16.

$$I_{xx} = 4 I_{yy} \tag{16}$$

$$\frac{bh^3}{12} = 4 \times \frac{b^3h}{12}, \quad h^2 = 4b^2 \text{ or } h = 2b$$

The value of $b=4 \text{ mm}$ was determined from Equations 13 and 15 then $h=8 \text{ mm}$.

2.8 Carrot washing and grading drum design

The drum is a cylinder into which water is pumped into it through a perforated hollow shaft to wash and grade carrots tubers into desired quality and sizes. It rotates at the desired speed for the purpose using a sprocket and chain configuration. Carrots could be loaded through the door. The mass of the drum (washing and grading unit) (M_D), the mass of unwashed and ungraded carrot (MC), the drum diameter (D), and the actual volume of the drum (V_D) are all critical for optimal operation and achieving the desired outcomes. The mass of the washing and grading unit (M_D) was calculated using Equation 17 using the volume of the washing and grading cylindrical unit (V_D) and the density of the Eucalyptus tree 398 kg m^{-3} used to construct the Drum.

$$M_D = \rho V_D \tag{17}$$

Dereje (2019) computed the volume of the washing and grading cylindrical unit (V_D) by subtracting the total volume of the holes or slots (V_s) from the total volume of

the solid cylindrical washing and grading unit (V_{solid}) using Equation 18.

$$V_D = V_{solid} - V_s \quad (18)$$

The complete solid drum should be filled 1/4 to 1/6, or 4 to 6 times the volume of unwashed and ungraded carrots, for better washing and grading (Anjali and Ikhar, 2018). For hand-cranking machines, the ideal capacity of the

drum for washing and grading was around 10 kg to 15 kg per charge, as reported by many scholars in various types of literature. For developing this machine based on the recommendation above, $MC=10$ kg, the volume of the drum was taken as 6 times the volume of unwashed and ungraded, and its capacity was taken as 10 kg per one charge.

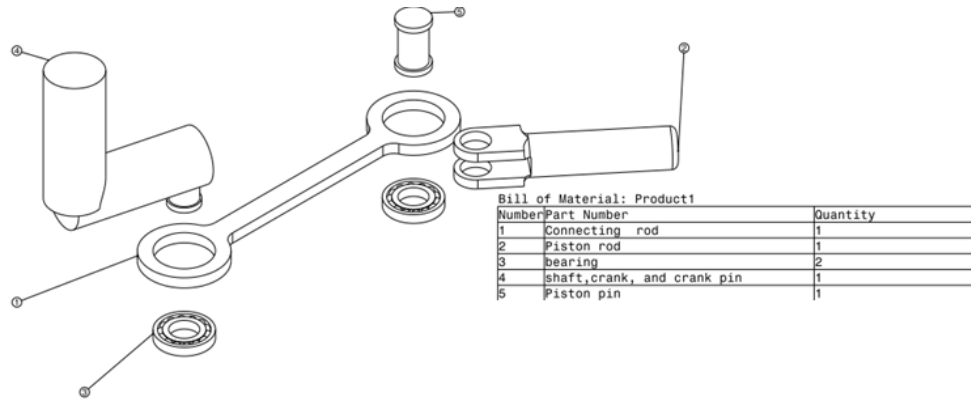


Figure 3 Connecting rod assembly and crank mechanism

Because of the bulk density of the observed carrot samples was 500 kg m^{-3} , the volume of unwashed and ungraded carrots, as well as the inner diameter of the washing and grading drums, were calculated using the aforementioned data and the volume, density, and mass connection as indicated by Equations 19 and 20.

$$V_{solid} = 6 \times V_{Carrot} \quad (19)$$

where, V_{solid} is the volume solid washing and grading drum

V_{Carrot} = the volume of unwashed and ungraded carrots (0.02m^3)

$$V_{Carrot} = \frac{m}{\rho} \quad (20)$$

where, m is the mass of unwashed and ungraded carrots (kg), ρ is the bulk density of unwashed and ungraded carrots (kg m^{-3}).

$$\therefore V_{solid} = 6 \times 0.02\text{m}^3 = 0.12\text{m}^3$$

The volume of the slot is calculated using Equation 21, which is equal to the volume of the slot in the washing unit (V_{ws}) plus the volume of the slot in the grading unit (V_{sg}) (Dereje, 2019).

$$V_s = V_{ws} + V_{sg} \quad (21)$$

In the washing unit, the space between the wood planks

was 2 mm to allow only water with impurities to get through, while in the grading unit, the spacing between timbers was increased gradually to perform rough grading. It was designed based on the geometric mean diameter of carrot root. The carrot root less than 40 mm GMD were graded as their size in grading unit, while carrots with diameters greater than 40 mm were graded at the cylinder outport which are recommended for far markets. To achieve the above stated result, wood planks with a length of 1.5 meters and a thickness of 20 millimeters were chosen to allow enough time for washing and grading. The lengths of the washing and grading units were 0.7 m and 0.8 m, respectively (see Figure 4 and Figure 6).

The volume of slot (V_{ws}) in washing unit determined using Equation 22 from the geometry of Figure 4 (Dereje, 2019).

$$V_{ws} = LWTn \quad (22)$$

$V_{ws} = 700\text{mm} \times 1\text{mm} \times 20\text{mm} = (1.40 \times 10^5\text{mm}^3) \times n$, Where, L is the length of slot in washing unit (mm), W is the width of slot in washing unit (mm), T is the thickness of timber in the washing unit (mm), and n is the number of root.

As illustrated in Figure 6, the slots are trapezoidal in

shape, with a width of 2 mm at the end of the washing section and 30 mm at the outport. As a result, its volume (V_{sg}) is calculated using the trapezium volume formula (Equation 23) (Khurmi and Gupta, 2005).

$$V_{sg} = \left(\frac{1}{2} b_t h_t t + b_r h_r t \right) n \quad (23)$$

where, b_t is the base of the triangular parts of the trapezoidal slot (mm), b_r is the base of the rectangular parts of the trapezoidal slot (mm), h_t is the height of the triangular parts of the trapezoidal slot (mm), h_r is the height of the rectangular parts of the trapezoidal slot (mm), t is the thickness of the grading cylinder that makes the Timber (mm), and n is the number of slots.

$$V_{sg} = (1/2 \times 800 \text{ mm} \times 29 \text{ mm} \times 20 \text{ mm} + 800 \text{ mm} \times 2 \text{ mm} \times 20 \text{ mm}) \times n$$

$$V_{sg} = (3.23104 \text{ mm}^3) \times n$$

The number of slots was calculated by dividing the solid circumference of the washing and grading cylinder by the sum of the width of the timber and the gap between the timber at the washing unit, as indicated by Equation 24. Because the width of the timbers in the washing machine is the maximum and the slots are the smallest, the width of the timbers is the maximum and the slots are the smallest (Dereje, 2019).

$$n = \frac{\pi d_i}{w_i + c_i} \quad (24)$$

where, n is the total number of timber, d_i is the inner diameter of washing and grading unit (Drum) (mm), w_i is the width of timber at washing unit (mm), and c_i is the gap size in washing unit (mm).

$$n = \frac{\pi d_i}{65 \text{ mm} + 2 \text{ mm}} = 0.05 \text{ mm} \times d_i$$

The cylinder volume formula (Equation 25) is used to calculate the volume of the solid hollow cylinder (V_{solid}) from the inside diameter (d_i) and length of the cylinder (L) (Khurmi and Gupta, 2005; Umani and Markson, 2020).

$$V_{solid} = \frac{\pi d_i^2 L}{4} \quad (25)$$

$$\begin{aligned} \therefore V_{solid} &= \frac{\pi \times d_i^2 \times 1500 \text{ mm}}{4} = 1178.10 \text{ mm} \times d_i^2 \\ &= 1.18 \text{ m} \times d_i^2 \end{aligned}$$

Therefore, the diameter of the washing and grading cylinder was determined equalizing the Equation 20 and 25 as follows.

$$0.12 \text{ m}^3 = 1.18 \text{ m} \times d_i^2, d_i = 0.32 \text{ m} = 320 \text{ mm} \therefore n = 0.05 \text{ mm} \times 320 \text{ mm} = 15 \text{ mm}^2$$

After the value of n determined, V_{ws} and V_{sg} calculated according to Equations 22 and 23 which were $2.10 \times 10^{-3} \text{ m}^3$ and $4.85 \times 10^{-4} \text{ m}^3$ respectively.

Therefore, using Equations 22, 19, 18 respectively, the value of $V_s = 2.59 \times 10^{-3} \text{ m}^3$, $V_D = 0.117 \text{ m}^3$, and $W_D = 458.43 \text{ N}$ were estimated.

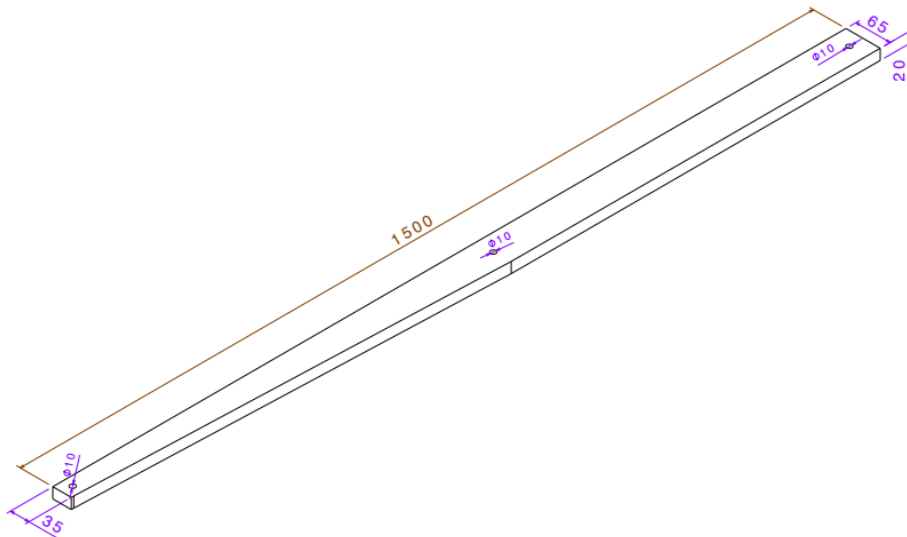


Figure 4 Isometric view of timber (all dimensions are in mm)

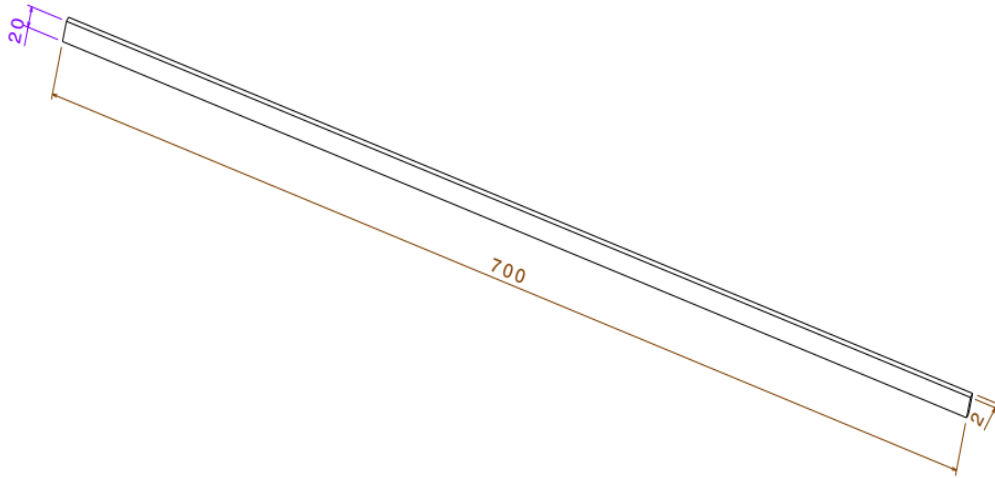


Figure 5 Isometric view of slot in washing unit(all dimensions in mm)

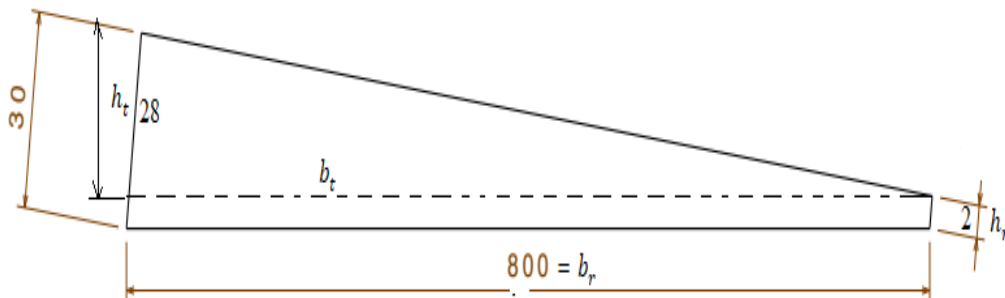


Figure 6 The shape of slot in grading unit(all dimensions in mm)

2.9 Shafts design

2.9.1 Transmission shaft design

The transmission shaft is the shaft that gets power from the pedal via the chain and transmits it to the drum shaft via belts for simultaneous washing and grading water pumping. As illustrated in Figure 8, the smaller sprocket (driven pinion) was equipped with a bearing using an interference fitting technique, while the transmission shaft was fitted with a bearing using a clearance fitting approach. Because it is bent and twisted by chain tension, belt tension, and Crank tangential force, this shaft is subjected to torsion and bending pressures.

The torque exerted by the sprocket is equal to that exerted by the transmission shaft as related by Equation 26 (Gujar and Bhaskar, 2013).

$$\tau_{Sprocket} = \tau_{Transmission\ shaft} \quad (26)$$

where, $\tau_{Sprocket}$ is the torque exerted by sprocket and $\tau_{Transmission\ shaft}$ is the torque exerted by transmission

shaft.

The value of transmission shaft torque was obtained from the power formula developed by Equation 27 as (Patil et al., 2021).

$$\tau_{Sprocket} = \frac{60P}{2\pi N_{Sprocket}} \quad (27)$$

where, P is the input power in W, $\tau_{Sprocket}$ is the torque exerted by sprocket (4.42 N), and, $N_{Sprocket}$ is the angular speed of sprocket (11.31 m s⁻¹).

The torque exerted by the transmission shaft and crank (N m) were calculated as given by Equations 28 and 29 (Patil et al., 2021; Sharma and Mukesh, 2010).

$$T_{Transmission} = T_{Belt} - T_{crank} \quad (28)$$

$$T_{crank} = F_T r \quad (29)$$

where, $T_{Transmission}$ is the torque exerted by transmission shaft, T_{Belt} is the torque exerted by belt, T_{crank} is the torque exerted by the crank, F_T is the crank tangential force, and r is the crank radius (190 mm) because the crank radius is half of the piston stroke.

The net force applied on the crankpin or Crank

tangential force was determined by Equation 30 (Guru et al., 2019).

$$F_T = F_C \sin(\theta + \phi) \quad (30)$$

where, F_C is the force acting along the piston rod, ϕ is the angle of inclination of the connecting rod with the

line of stroke, and θ is the angle of inclination of the crank from top dead center.

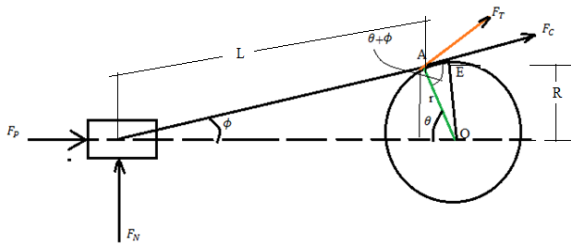


Figure 7 Net force applied on the crankpin and piston effort

As previously stated, the maximum value of F_C force along the connecting rod is used to construct the connecting rod. The angle of inclination of the connecting rod with the line of stroke ($\phi = 19.47^\circ$) obtained using sine law as given by Equation 31 for the maximum $F_C=500$ N, $r=OE$, and $OE=R$ as seen from the geometry of the picture above.

$$\frac{\sin \phi}{R} = \frac{\sin \theta}{L} \quad (31)$$

$$\phi = \sin^{-1} \left(\frac{R \times \sin \theta}{L} \right)$$

$$\phi = \sin^{-1} \left(\frac{25\text{mm} \times \sin 90^\circ}{75\text{mm}} \right) = 19.47^\circ$$

where, L is the length of connecting rod (75 mm) and R is the radius of crank (25 mm) when $\theta = 90^\circ$.

$$\therefore F_T = 500 \text{ N} \times \sin(109.47^\circ) = 471.40$$

$$, T_{crank} = 471.40 \text{ N} \times 0.03\text{m} = 11.79 \text{ Nm},$$

$$T_{Belt} = 4.42 \text{ Nm} + 11.79 \text{ Nm} = 16.21 \text{ Nm}$$

In another scenario, the torque exerted on the driving pulley was determined as Equation 32 because the effective turning (driving) force at the circumference of the driven pulley or follower is the difference between the two tensions (Patil et al., 2021).

$$T_{Belt} = (T_1 - T_2)r_1 \quad (32)$$

$$(T_1 - T_2) = 426.45\text{N}$$

where, r_1 is the the radius of the driving pulley (radius of transmission shaft pulley) (0.038 m), T_{Belt} is the torque

exerted on the driving pulley (16.21 N m), T_1 is the tension in the tight side of the belt (N), and T_2 is the tension in the slack side of the belt (N).

Equation 33 was used to calculate the relationship between the tight side (T_1) and slack side (T_2) tensions of a V-belt belt in terms of coefficient of friction (μ) and angle of contact (θ)(Umani and Markson, 2020).

$$\frac{T_1}{T_2} = e^{\mu\theta} \quad (33)$$

The angle of contact or lap at the Smaller pulley (θ) was computed using Equation 34 for an open belt with both pulleys made of the same material (Patil et al., 2021).

$$\theta = \left(180^\circ - 2 \times \sin^{-1} \left(\frac{D-d}{2C} \right) \right) \frac{\pi}{180} \text{ rad} \quad (34)$$

where, θ is the angle of contact or lap at the smaller pulley, D is the diameter of larger pulley (Diameter of Idler Shaft Pulley) (m), d is the diameter of smaller pulley (Diameter of Transmission Shaft Pulley)(m), and C is the center distance between transmission shaft pulley and idler shaft pulley .

$$\theta = \left(180^\circ - 2 \times \sin^{-1} \left(\frac{0.14\text{m} - 0.075\text{m}}{2 \times 0.183\text{m}} \right) \right) \frac{\pi}{180} \text{ rad}$$

$$= 2.78 \text{ rad}$$

Because the chosen pulleys were made of cast iron and the belts were made of rubber, the coefficient of friction between cast iron and rubber is 0.30. Therefore, the Equation 33 was modified as $T_1=2.31T_2$. substituting the value of T_1 into Equation 32, T_2 was 325.5 N. by multiplying T_2 with 2.31 the value of T_1 calculated as 751.90 N. Another significant component of the transmission shaft is the chain tension, which was calculated using Equation 35 and the Chain velocity (Pitch line velocity of the smaller sprocket), which was measured using Equation 36 (Adzimah and Agbovi, 2015).

$$P = T_C V_C \quad (35)$$

where, T_C is the chain tension and V_C is the velocity of chain.

$$V_C = \frac{TpN}{60} \quad (36)$$

where, N is the speed of smaller sprocket (m s^{-1}), T is the number of teeth on the sprocket, and p is the pitch of

the chain in meters.

$$V_C = \frac{20 \times 0.009525m \times 108 \text{ rpm}}{60} = 0.34 \frac{m}{s}$$

$$\therefore T_C = \frac{50W}{0.34 \frac{m}{s}} = 147.06N$$

The chain attached to the shaft with 30° from vertical line, therefore the chain tension applied to the shaft in vertical and horizontal components as following

$$T_{cv} = T_C \cos 30$$

$$T_{cv} = 127.36N$$

$$T_{ch} = T_C \sin 30$$

$$T_{ch} = 72.91N$$

where, T_{cv} is the chain tension of vertical component in N and T_{ch} is the chain tension of horizontal component in N.

The mass of the transmission shaft pulley, smaller

sprocket, crank, and chain were measured using beam balance at 0.25 kg, 0.12 kg, 0.02 kg, and 0.41 kg, respectively. At the same time, the vertical component of chain tension is caused by sprocket weight and the crank tangential force is caused by crank weight pushing on the shaft vertically downward. As a result, they were treated as a single force in the following way.

$$T_{cvs} = T_{cv} + W_s = 127.36N + 1.18N = 128.54F_{TW}$$

$$= F_T + W_{Crank} = 471.40 N + 0.2 N$$

$$= 471.60 N$$

where, T_{cvs} is the summation of the vertical component of chain tension and sprocket weight, F_{TW} is the summation of crank tangential force and weight of the crank.

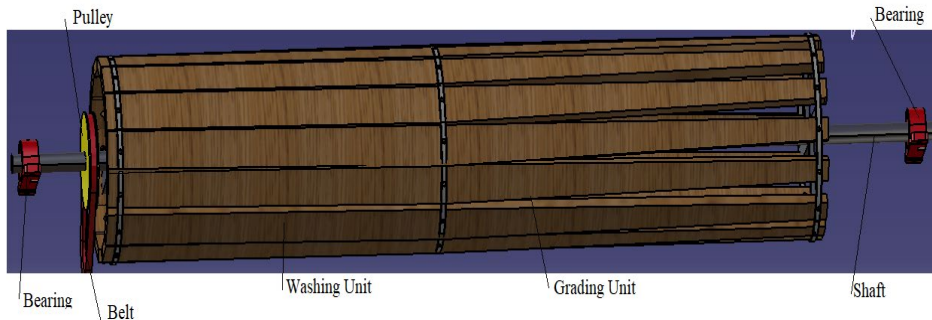


Figure 8 Carrot washing and grading machine drum assemblies modeled by CATIA V5

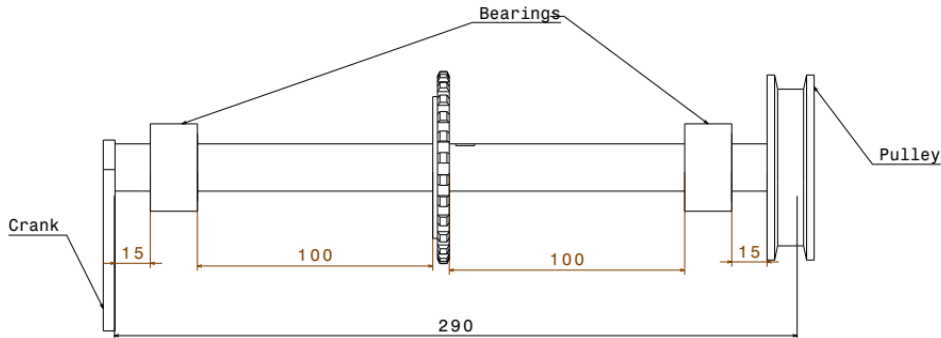


Figure 9 Transmission assembly(all dimensions in mm)

The belt tensions and the pulley's weight both act at the same location but in opposite ways in this situation. The tensions are increasing and the pulley weight is decreasing. Because the stresses were more than the pulley's weight, they were reinterpreted as succeeding.

$$T = T_1 + T_2 - W_p = 1077.41 N - 2.45 N = 1074.96N$$

The shaft was supported by two bearings at locations

B and D, as indicated in Figure 10. The bearing B is 15 mm distant from the crank, and the bearing D is 15mm apart from the pulley. However, because the forces and weights are applied from the center of the pulley, sprocket, and crank, the bearing B is 30 mm and 113.5 mm apart from the crank center and sprocket center, respectively. In the same way, bearing B is 35 mm and 113.5 mm distant from the center of the pulley and the

center of the sprocket, respectively. There is a response force at each support that balances the shaft's twisting and bending. As a result, the response at each support must be determined before twisting and bending moments can be calculated.

To determine the reaction at B point for vertical components, the moment about point D was taken as M_{Dy} as Equation 37 (Khurmi and Gupta, 2005).

$$+\circlearrowleft \sum M_{Dy} = 0 \tag{37}$$

Where $+\circlearrowleft$ indicates that the rotation of the moment in the anticlockwise direction is positive and negative in the clockwise direction

As seen from Figure 11, the maximum bending momentum on the vertical plane (M_{Dy}) calculated as (-43 N m).

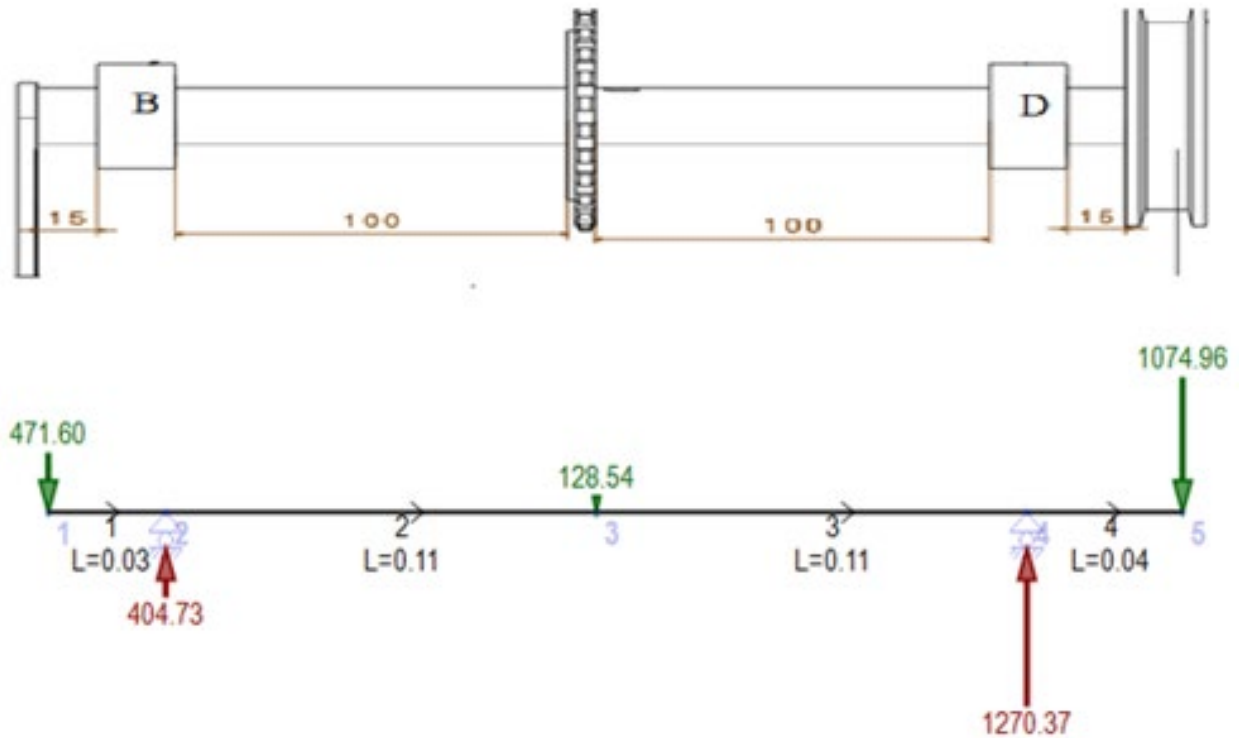


Figure 10 Transmission shaft loading diagram on the vertical plane (All dimensions in m and all forces in N)

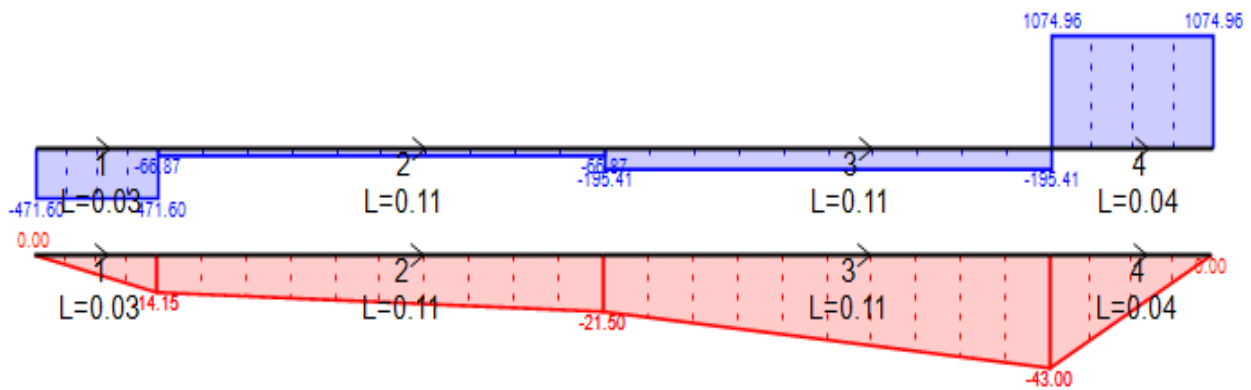


Figure 11 Shear force and bending moment diagram on the vertical plane

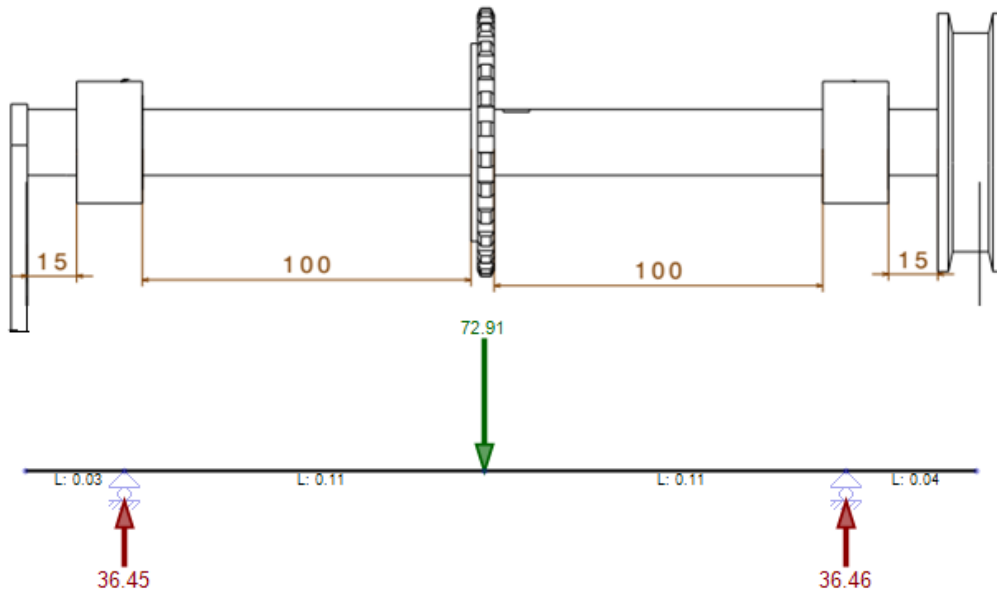


Figure 12 Transmission shaft loading diagram on the horizontal plane(All dimensions are in m and all forces are in N)

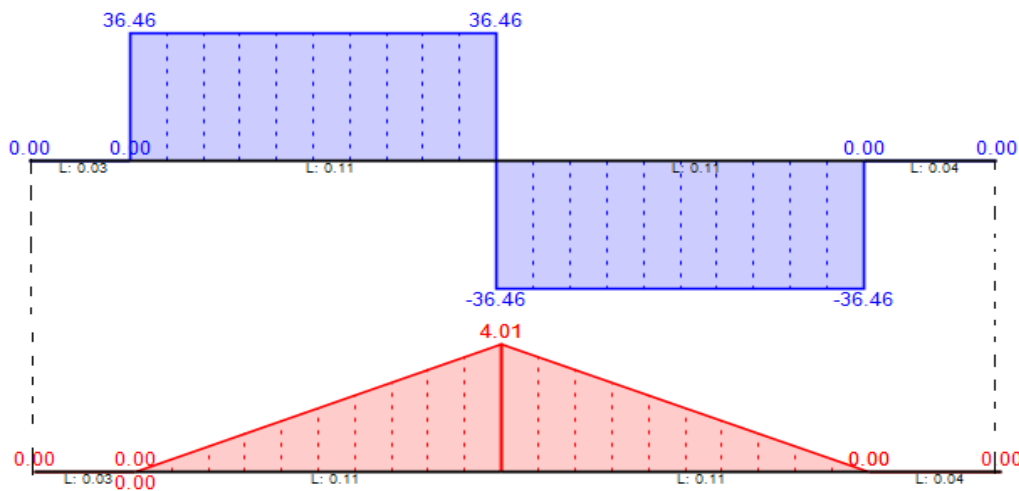


Figure 13 Transmission shaft shear force and bending moment diagram

The moment around point D is taken as MDx in the same scenario to determine the reaction at B point for horizontal components (Khurmi and Gupta, 2005).

The resultant bending moments on the shaft can be determined by taking all values in mx and my and the maximum one selected as Equation 38 (Khurmi and Gupta, 2005).

$$M_b = \sqrt{M_y^2 + M_x^2} \tag{38}$$

where, Mb is the resultant bending moments (N m), My is the maximum bending moments on the vertical plane (N m), and Mx is the maximum bending moments on the horizontal plane (N m).

It was seen that bending moment was maximum at D, therefore, the maximum bending moment, $M_m = M_D = 43 \text{ N m}$.

As previously stated, a transmission shaft is a shaft that is subjected to varying torque and bending moments. Equations 39, 40, 41, and 42 and Km & Kt 1 to 3 were used to compute the equivalent twisting and bending moments for rotating shafts (Guru et al., 2019; Patil et al., 2021).

$$T_e = \sqrt{K_t T^2 + k_m M_m^2} \tag{39}$$

$$T_e = \tau d^3 \frac{\pi}{16} \tag{40}$$

and equivalent bending moment,

$$M_e = \frac{1}{2} (k_m M_m + T_e) \tag{41}$$

$$M_e = \frac{\pi d^3}{32} \sigma_b \quad (42)$$

where, T_e is the equivalent twisting moment, K_m is the combined shock and fatigue factor for bending, τ is the torsional shear stress, σ_b is the bending stress and K_t is the combined shock and fatigue factor for torsion, T is the twisting moment of the shaft, M is the bending moment, and M_e is the equivalent bending moment.

$$T_e = \sqrt{K_t T^2 + k_m M_m^2}$$

$$\tau_{Transmission\ shaft} = T = 4.42 Nm, k_t = 3, k_m = 1,$$

$$\text{and } M_m = M_D = 43 N m$$

$$T_e = \sqrt{58.61 N^2 m^2 + 1849 N^2 m^2} = 43.68 N m$$

According to the American Society of Mechanical Engineers (ASME) code for the design of transmission shafts, $\tau = 42 \text{ MPa} = 42 \text{ N mm}^{-2}$ and $\sigma_b = 84 \text{ MPa} = 84 \text{ N mm}^{-2}$ for shafts with allowance for keyways (Hakizimana et al., 2020).

$$T_e = \tau d^3 \frac{\pi}{16} \quad d = \sqrt[3]{\frac{16 \times T_e}{\tau \pi}} = 17.43 mm$$

$$M_e = \frac{1}{2} (k_m M_m + T_e) = 43.34 Nm$$

$$d = \sqrt[3]{\frac{32 \times 43.34 \times 1000}{84 N/mm^2 \pi}} = 17.39 mm$$

Therefore, the diameter of the transmission shaft was determined to 18mm which is the standard size near to calculated value.

2.9.2 Idler shaft design

The idler shaft was necessary to reduce the rotational speed of the transmission shaft 11.31 m s^{-1} to washing and grading drum speed 1.47 m s^{-1} , as assumptions made under section 2.4 It is supported by two pulleys and two supporting bearings. A rubber belt connects the driver transmission shaft pulley (75 mm) to the idler shaft-driven pulley (140 mm), and the idler shaft driver pulley (75 mm) to the main (drum) shaft-driven pulley (155 mm). As illustrated in Figure 14, the two bearings were attached to the frame column, allowing the shaft to pass through the frame column and the bearings to hold the pulleys at either edge.

The torque exerted by the idler shaft on other assemblies is the first parameter used to compute its diameter (Equation 43)(Sharma and Mukesh, 2010).

$$\frac{D_2}{D_1} = \frac{\tau_{Idler}}{\tau_{Transmission\ shaft}} \quad (43)$$

where, D_1 is the transmission shaft driver pulley (m), D_2 is the idler shaft-driven pulley (m), τ_{Idler} is torque exerted by idler shaft (Nm), and $\tau_{Transmission\ shaft}$ is the torque exerted by the transmission shaft (Nm).

$$\frac{0.140m}{0.075m} = \frac{\tau_{Idler}}{4.42Nm}, \quad \tau_{Idler} = 8.25Nm$$

In another situation, the torque exerted on the driver and driven idler shaft pulley were calculated using the principle of Equations 32 to 35 and the value of tensions due belt on the driver and driven idler pulleys were calculated as 122.28 N and 572 N respectively.

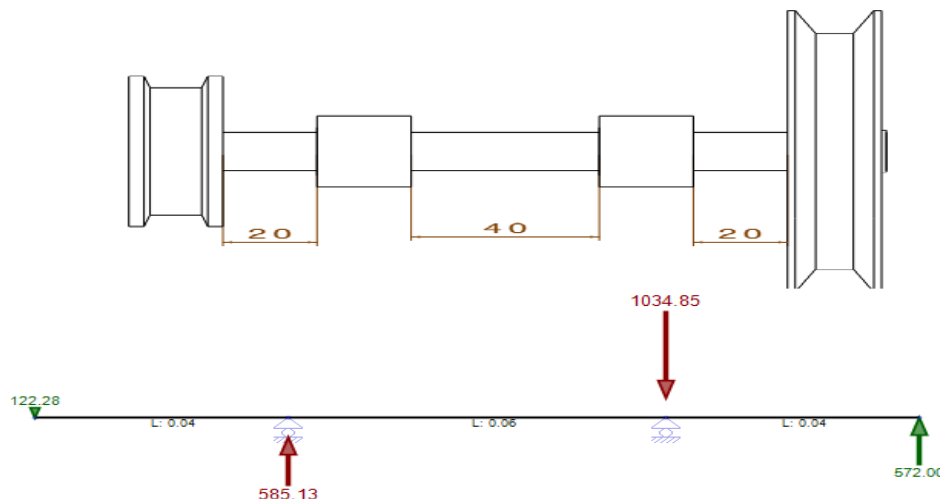


Figure 14 Idler shaft loading diagram on the vertical plane (all dimensions in m and all forces in N)

The instant about point 3 was taken as M_{3y} according to Equation 44 to determine the reaction at two points (R_2) (Umani and Markson, 2020)

$$+\curvearrowright \sum M_{3y} = 0 \tag{44}$$

$$R_2 = \frac{35.11Nm}{0.06m} = 585.13N...$$

Where $+\curvearrowright$ indicates that the rotation of the moment in the anticlockwise direction is positive and negative in the clockwise direction

The summation of forces in the vertical direction (FV) is zero at equilibrium. As a result, the equilibrium equation was used to determine the reaction at point 3 (R_3).

$$+\downarrow \sum F_v = 0$$

Where, $+\downarrow$ denotes that the downward shear forces are positive and the upward shear forces are negative.

$$T - R_2 + R_3 - T_i = 0$$

$$R_3 = -122.28N + 585.13N + 572N = 1034.85N$$

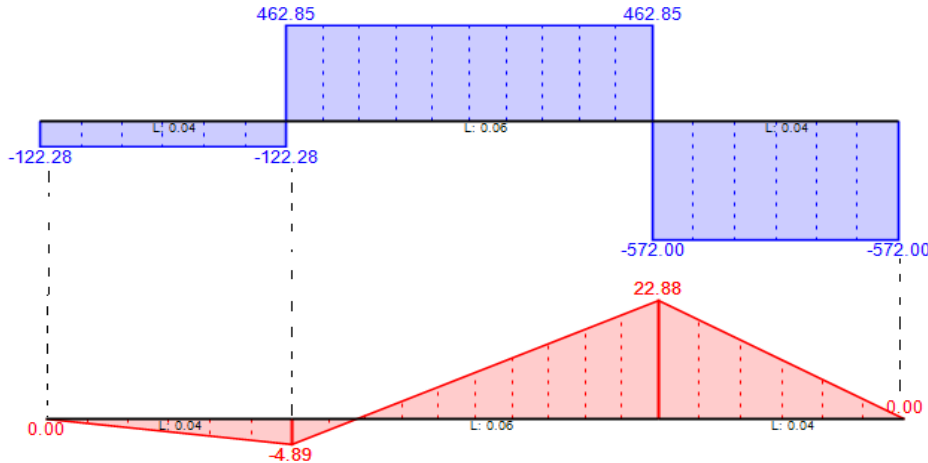


Figure 15 Shear force and bending moment diagram of idler shaft on the vertical plane

The bending moment was highest at point 3, which was 22.88 N m. The idler shaft is another type of shaft that experiences variable torque and bending moments. Using Equations 39 to 42, the corresponding twisting ($T_e=83.26$ N m) and bending moments of the idler shaft were determined in the same way as the transmission shaft. To design the shaft with allowance for keyways and subject to twisting moment, the shear and bending stresses are 42 MPa and 84MPa, respectively, as indicated in the section above.

$$d = \sqrt[3]{\frac{32 \times M_e}{\sigma_b \pi}} = 21.56mm \approx 20mm$$

$$d = \sqrt[3]{\frac{16 \times T_e}{\tau \pi}} = 21.59mm \approx 22mm$$

Therefore the diameter of the idler shaft was also determined to be 20 mm because 20 mm is the standard bearing size near 21.56 mm.

2.9.3 Drum shaft design

The mass of the washing and grading cylinder (M_D), the maximum mass of carrot root feed (M_C), the mass of the pulley, and belt tensions all operate on the drum shaft.

$$T_e = \tau d^3 \frac{\pi}{16}$$

$$M_e = \frac{1}{2}(k_m M_m + T_e)$$

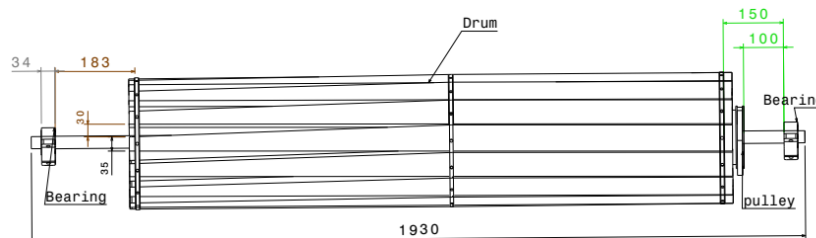


Figure 16 Washing and grading drum (all dimensions are in mm)

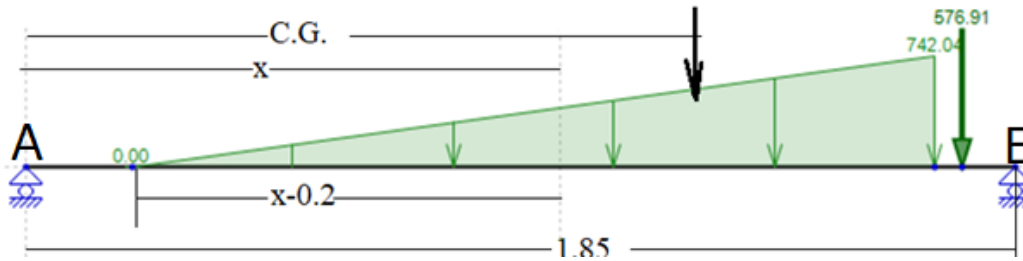


Figure 17 Drum shaft load diagram

The tensions ($T=58.3$ kg) and the mass of the pulley ($MP=0.5$ kg) act downward in a single point, and M_C and M_D act as a single force. $M_p+T=58.8$ kg and $M_D+M_C=56.7$ kg, respectively. The load applied to the shaft by the product and Drum is triangular uniform because the load applied by the product is high in the washing unit and low in the grading unit. According to Equation 45, the load operating on the Shaft in Washing and grading units is the area under the triangle, which is the distributed load (w) divided by two, that is $(wL/2)$ (Umani and Markson, 2020). As the triangular load (w) is acting straight down, the horizontal reaction (A_x) is zero.

$$\frac{wL}{2} = M_D + M_C \quad (45)$$

$$w = \frac{2(M_D + M_C)}{1.5m} = 75.64 \frac{kg}{m}$$

Where w =the distributed load triangular load ($kg\ m^{-1}$)

$M_D + M_C$ =the sum of the weight of the drum and unwashed and ungraded carrot (kg)

L =length of Drum (m)

The center of gravity (C.G.) of the triangle lies a distance of $\frac{2}{3} \times L$ from the apex.

$$i.e. C.G. = \frac{2}{3} \times 1.5m = 1m$$

To determine the reaction at E point (R_E), the moment about point A was taken as M_{Ay} according to Equation 46 (Khurmi and Gupta, 2005; Umani and Markson, 2020)..

$$+\curvearrowright \sum M_{Ay} = 0 \quad (46)$$

$$(1.85m \times R_E) - (1.75m \times 576.91N) - ((0.2m + 1m) \times 556.53N) = 0$$

$$R_E = 906.72N...$$

Where $+\curvearrowright$ indicates that the rotation of the moment in the anticlockwise direction is positive and negative in the clockwise direction

At equilibrium, the summation of forces on the vertical direction (F_v) is zero. Consequently, the reaction at point 1 (R_1) was determined from the equilibrium equation.

$$\sum F_v = 0$$

$$R_A = 556.53N + 576.91N - 906.72N = 226.72N$$

The symbol $+\downarrow$ denotes that the downward forces are positive and the upward forces are negative.

Shear forces at each point were calculated as follows

$+\downarrow V_y$ = shear force at x distance from point 1 to the required point.

$$V_A = 226.72N, V_B = 226.72N, V_C = 226.72N - 556.53N = -329.81N, V_D = -329.81N - 576.91N = -906.72N, V_E = -906.72N + 906.72N = 0$$

The symbol $+\downarrow$ denotes that the downward shear forces are positive and the upward shear forces are negative.

The direction of V_B and V_C are opposite, that means there is a point where the Shear force becomes zero between point B and C. Let's take section xx at distance x from point A between B and C at which $V_x=0$.

$$V_x = R_A - \text{area of section}$$

$$0 = R_A - \frac{1}{2}bh, b = x - 0.2m$$

$$0 = 226.72N - \frac{1}{2}(x - 0.2m)h \quad (47)$$

By similar triangle law

$$\frac{742.04N}{1.5m} = \frac{h}{x-0.2m}$$

$$h = 494.69N(x - 0.2m) \quad (48)$$

By substituting equation (48) into (47)

$$247.35N(x - 0.2m)(x - 0.2m) = 226.72N,$$

$$x = 1.16m$$

Therefore, the shear force is zero at a distance of 1.16m from supporter A or $x - 0.2m = 0.96m$ from point B.

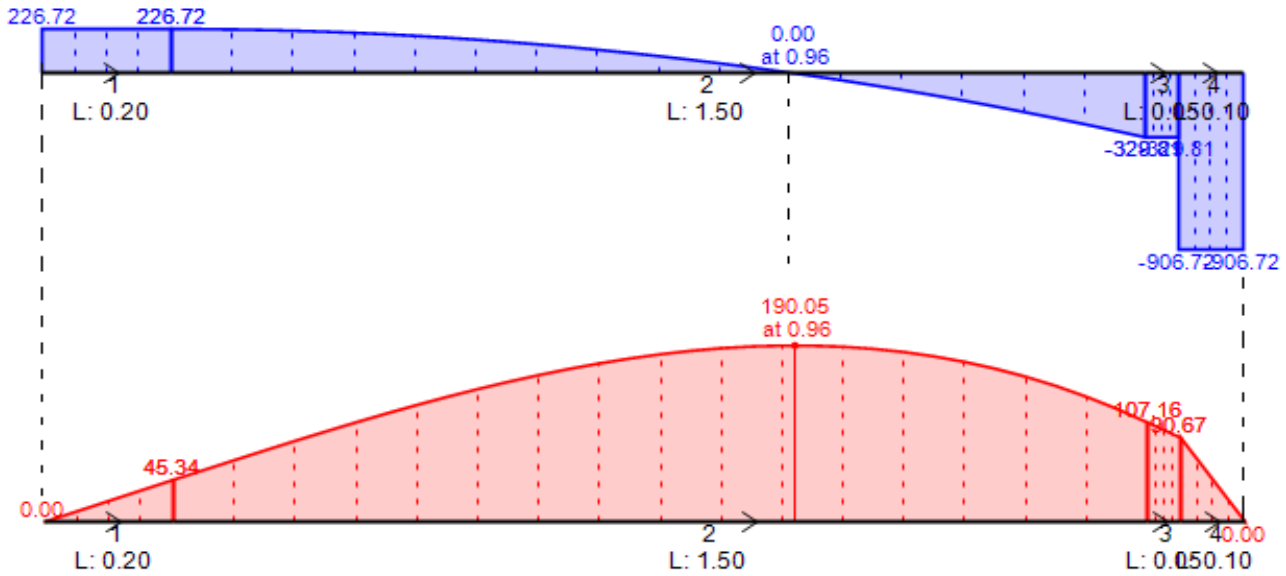


Figure 18 Shear force and bending moment diagram of the drum shaft on the vertical plane

The bending moment on the drum shaft as a result of the Equation 40 was also calculated and the maximum bending moment was 190.05 N m at point x, i.e. $M_m=190.05$ N m. Drum shafts are hollow shafts with perforated holes that are used to transmit water from the washing drum and are subjected to variable torque and bending forces. Equations 39 to 42 were used to compute the equivalent twisting and bending moments of the Drum shaft in the same way that they were calculated for transmission and idler shafts.

$$\tau_{Drum} = 8.25Nm \times \frac{0.155m}{0.075m} = 17.05Nm,$$

$$d = \sqrt[3]{\frac{16 \times T_e}{\pi \tau}} = 28.57mm \approx 30mm$$

$$M_e = \frac{1}{2}(k_m M_m + T_e),$$

$$d = \sqrt[3]{\frac{32 \times M_e}{\sigma_b \pi}} = 28.51mm \approx 30mm$$

Therefore the diameter of the idler shaft was also determined to be 30mm according to the above procedures.

2.10 Bearings selection

A bearing is a machine component that limits relative motion between moving elements to that which is desired. The static load carrying capacity, bearing life, dynamic load-carrying capacity, equivalent dynamic load, and load life relationship are some of the elements that should be

considered during bearing selection. The shafts diameter serve to define the bore size of the bearings; and resulting axial and radial force acting on the shaft was estimated for selection of the kind of bearings from axial to radial load ratio using Equation 49 (Patil et al., 2021).

$$F_R = \sqrt{R_x^2 + R_y^2} \tag{49}$$

where, R_x is the maximum resultant force acting on a bearing at a given point on the horizontal plane (kN), R_y is the maximum resultant force acting on a bearing a given point on the vertical plane (kN), F_R is the maximum resultant radial reaction force on the bearings at a given point (kN),

Bearing number 200 and 204 were chosen for supporter A and B of the Transmission Shaft and for both supporters of the Idler shaft respectively after comparing the computed C for each bearing with the value given by the catalog based on the bore diameter. Finally, bearing number 206 was chosen for both the drum shaft's supporter E and A.

2.11 Frame design

The frame is the chaises of the machine on which all other components like drums, seat, handlebar, sprocket, chain, etc. are mounted. It was made strong enough to resist the maximum magnitudes of compressive, tensile, and impact forces and simultaneously support the other

parts of the machine fixed on it. As shown in Figure 19, this machine had the frame components such horizontal pedal supporting, vertical Seat and handle supporting, horizontal water pump supporting, inclined transmission shaft supporting horizontal idler shaft supporting horizontal Main shaft supporting, and machine base. These vertical, horizontal and inclined components were welded together to form a strong efficient frame.

The materials selected for all frame components were hollow square steel due to its availability and relatively it's low price. Except for the transmission shaft and idler shaft supporting that were constructed from 60mm × 60mm × 4mm steel due to, they support the bearing which fit in bored 50mm sized shaft that welded to frame, all remained frame components were constructed from mild steel having 40mm × 40mm × 3mm diameter.

The dimension of operator seat and base frame

components was built by modifying an existing bicycle frame. The dimension of other frame components was based upon the dimension of the Drum and position. The diameter of the cylinder was used to determine the horizontal distance between the vertical columns that determined to 0.4 m. The length of the frame (1.93 m) from inlet vertical columns to outlet vertical columns, were determined based on the length drum by considering unloading space between drum and drum shaft.

The length of vertical columns (1.1 m) at the inlet was determined based on appropriateness for loading, operating, and pump seats. The vertical columns at outlet length (0.7 m) were lowered in length than that of inlet components to allow the gradual movement of products from the inlet port to the outlet port of the cylinder based on measured static friction angle (18.5°). A raised frame would make sample loading and unloading easier.

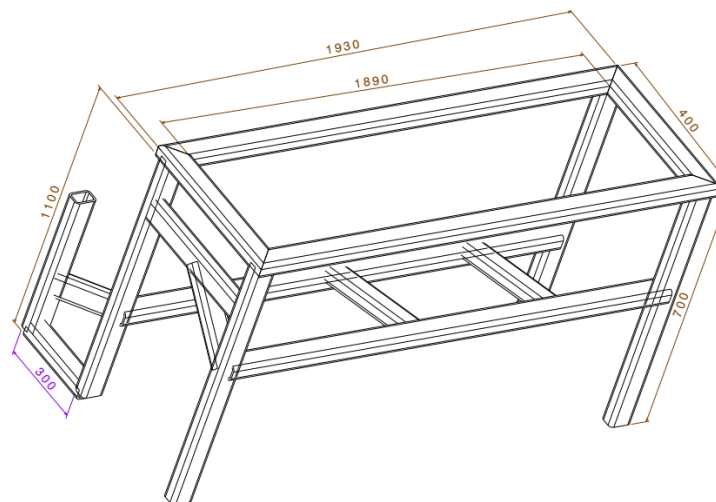


Figure 19 The frame (all dimensions are in mm)

2.12 Evaluation of carrot washing and grading machine

2.12.1 Preliminary evaluation

Preliminary evaluation was conducted without a load in the local workshop in Arsi Zone, Shirka District, Gobessa Town which is located at latitude and longitude of 07°37'N 39°30'E on august 2021. The evaluation conduct by visual observations and comparing specifications. During visual observation, the machine was set on the level area of the workshop and observed the operational condition and moving and rotating parts were observed, sound and any other factors such as vibration and shock were detected. In

the same case during the specification evaluation; the machine was kept on the level area and carefully the assembled and constructed parts were measured. Then the machine parts were cross-checked with designed specifications.

2.12.2 Performance indicator

Throughout capacity, washing efficiency, grading efficiency, and percentage of mechanical damages were determined using Equations 48-54 (Ambrose and Annamalai, 2013; Siddique et al., 2017; El-Rahman and Mosa, 2011; Umani and Markson, 2020; Dereje, 2019).

The machine throughout capacity of the carrot tubers washer and grader was determined based on the number of carrot roots washed and graded within a specified time as Equation 50.

$$C = \frac{m_{total}}{t} \tag{50}$$

where, C is the machine capacity (kg h^{-1}), m_{total} is the total mass of unwashed and ungraded sample (kg), and t is the time consumed in operation (h).

The washing efficiencies of the machine were determined by dividing the mass of the sample after washing by total mass sample by the total number of the sample as given by Equation 51.

$$we = \frac{m_{after}}{m_{total}} \times 100 \tag{51}$$

where, we is the washing efficiency (%) and m_{after} is the average mass of washed sample received at all outlets in kg.

Grading system efficiency was determined by taking the products of the efficiencies of grading small, medium, and large tubers and Equations 52, 53, 54, and 55 according to

$$Ge (\%) = (\eta_s \times \eta_m \times \eta_L) \times 100 \tag{52}$$

$$\eta_s = \frac{\text{mass of correctly graded small tuber}}{\text{Total mass of small tuber in the sample}} \tag{53}$$

$$\eta_m = \frac{\text{mass of correctly graded medium tuber}}{\text{Total mass of medium tuber in the sample}} \tag{54}$$

$$\eta_L = \frac{\text{mass of correctly graded larger tuber}}{\text{Total mass of large tuber in the sample}} \tag{55}$$

where, Ge is the grading system efficiency (%), η_s is the efficiency of grading smaller tubers, η_m is the

efficiency of grading medium roots and η_L is the the efficiency of grading large.

Damage of roots with abrasion after the washing and grading operation was considered. The percentage of damaged roots was taken by considering the total number of roots with abrasion after the operation against the total number of roots in the sample as indicated in Equation 56.

$$\text{Damaged roots}(\%) = \frac{\text{Total mass of root with abrasion}}{\text{Total mass of root in the sample}} \times 100 \tag{56}$$

3 Results and discussion

3.1 Time required to complete washing and grading activities

As Figure 20 shows, the cylinder speed has negative relation with time. As the drum rotation increase, the loaded carrot is forced to output quickly which reduce the time. Therefore, there was a highly significant reduction in time as the cylinder speed was increased. On the contrary, the feeding load has a positive relation to time. Because as the feed load increases the drum speed decreases this causes the elongation of time. Therefore, there was a highly significant increment in time as the feeding load was increased. The average minimum and maximum time to complete the washing and grading operation was recorded as 2 minutes and 10.88 as shown in Figure 20, respectively. It is better when compared to traditional washing and grading methods that need a minimum of 12 minutes for the same samples.

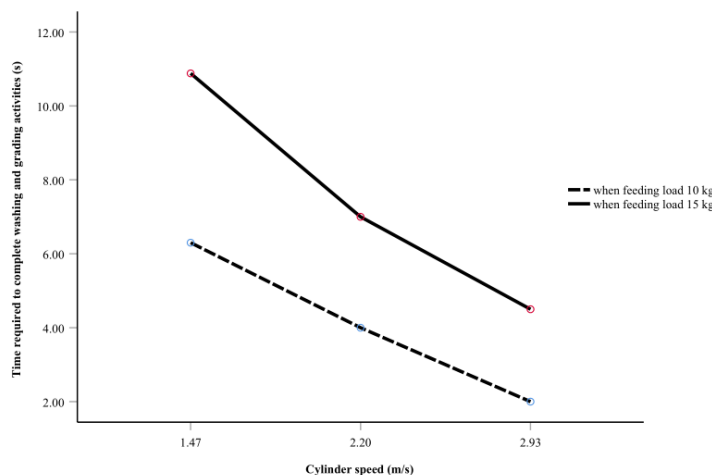


Figure 20 Effects of feeding load and of cylinder speed on the time required to complete washing and grading activities

3.2 Washing efficiency

Evaluation results indicated that the washing efficiency increased 91.13% to 98.70% for the range of the variable of speed between 1.47 to 2.93 m s⁻¹ during machine the operated with 10 kg feeding materials and 84.87% to 95.24% during machine operated with 15 kg feedings. This tendency showed the effect of drum speed and feeding load on the washing efficiency as shown by Figure 21. The washing efficiency gradually increases as the speed increases due to the high impact of the washing drum on the carrot tubers. And it is reduced as the feeding load increases due to the drum-free space becoming occupied with carrot tubers that protect water not to reaching each of the single products. Also, the water introduced to the drum

increased the washing efficiency based on the force of pedaling. If the operator increased pedaling force, crank rotation and cylinder speed have also increased. As the crank rotation and cylinder speed increased, enough water-induced to the washing drum and the high impact of the washing drum applied to root that was the reason for high washing efficiency.

Effect analysis for washing efficiency was highest (98.70%) at 2.93 m s⁻¹ cylinder speed and 10kg feeding load due to high impact and high water introduced to drum. This result is better than the results obtained by Ambrose and Annamalai (2013) and Amin and Hossain (2021) for the effect of speed drum on washing efficiency.

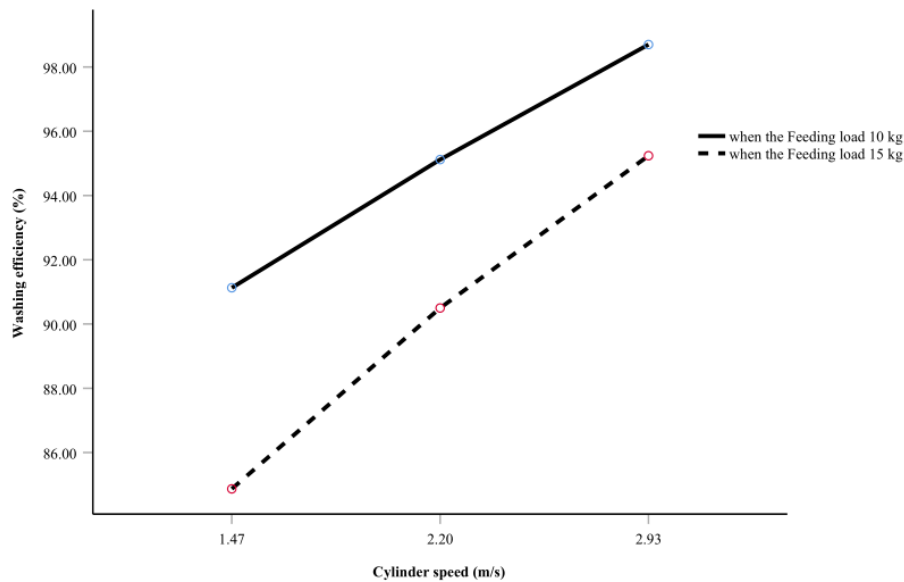


Figure 21 Effects of feeding load and cylinder speed on the washing efficiency

3.3 Grading efficiency

The grading efficiency ranges from 81.87% to 92.23% for the range of the variable of speed between 1.4-28 m s⁻¹ during machine the operated with 10 kg feeding materials and 72.89% to 80.86% during machine operated with 15 kg feedings. Figure 22 shows an inclining trend in the grading efficiency with the effect of cylinder speed and declined with the effect of feeding load. This trend is a result of the evaluation procedure of calculating the grading efficiency which is based on the ratio of the graded roots mass obtained from correctly graded roots in their

right outlet to total roots mass at the drum. From the test conducted more roots were obtained at the larger outlet (out port) as the speed increased from 1.47 to 2.93 m s⁻¹. This occurred as a result of the high drum speed, there is the probability of smaller roots passing way over their right outlet to the larger outlet. Unlikely, at a higher feeding load, the grading efficiency decreased gradually as is shown in Figure 22 because of the increased number of roots covering the right outlet and forcing it to the outer port. Due to that, there is a high probability of incorrectly grading products.

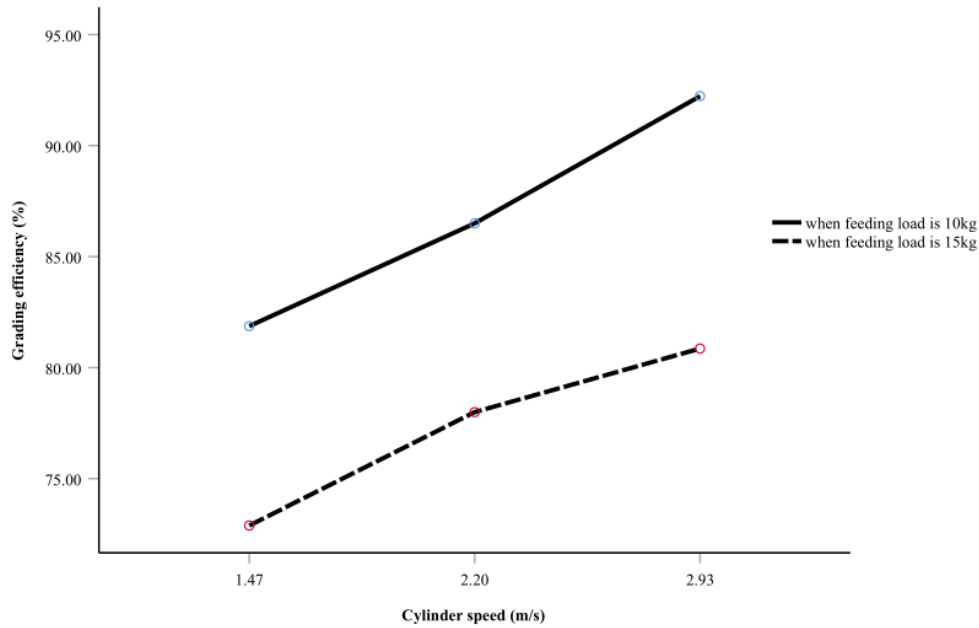


Figure 22 Effects of feeding load and cylinder speed on the grading efficiency

3.4 Roots damage

Figure 23 shows the effect of drum speed on root damage at different feeding loads. The result indicated that the percentage of root damage increased gradually from 1.05% to 3% with the increase in drum speed from 1.47-

2.93 m s⁻¹ and feeding load from 10 kg to 15 kg. The cylinder speed increases the root damage by creating a high impact on the roots. Root damage increased highly as the roots crowded with each other due to the high amount of feeding materials.

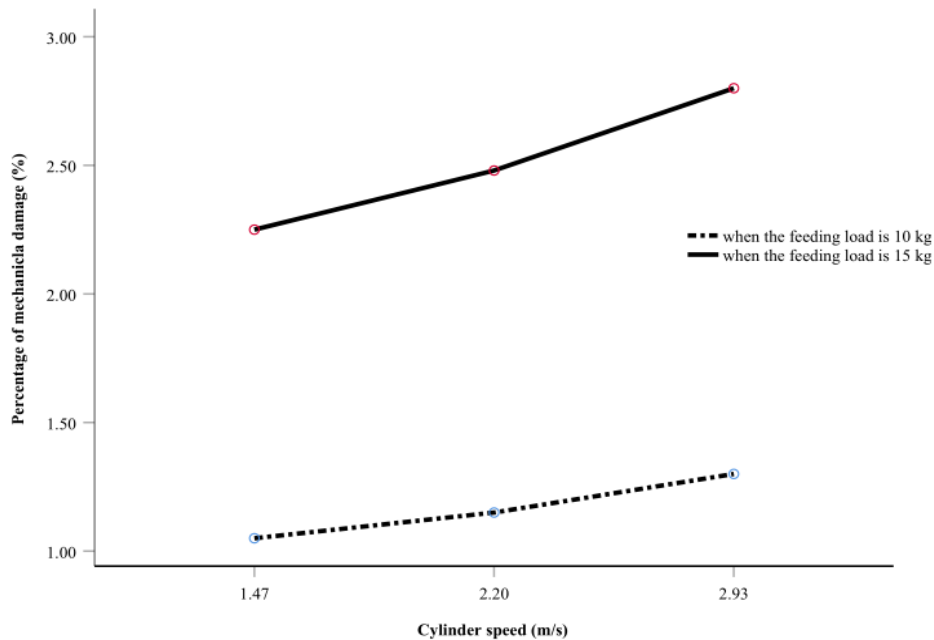


Figure 23 Effect of feeding load and cylinder speed on the percentage of damage root

3.5 Throughput put capacity

From Figure 24 it was observed that drum speed and the feeding load were proportional and inversely proportional to throughput put capacity respectively. The

highest throughput capacity 242.17 kg h⁻¹ was obtained at the highest cylinder speed (2.93 m s⁻¹) and lower feeding load (10 kg).

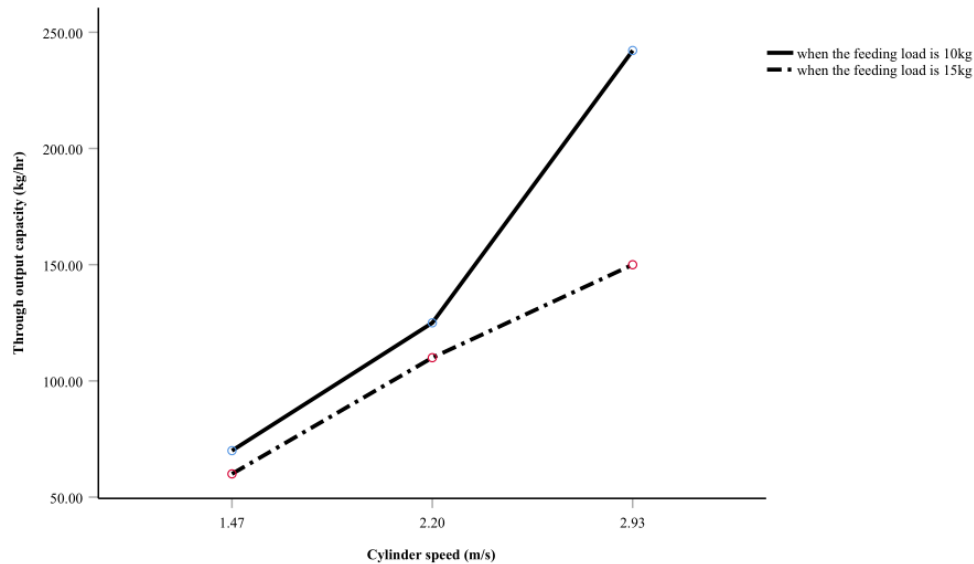


Figure 24 Effects of feeding load and cylinder speed on the throughput put

This trend is based on the fact that the small number of materials with the highest cylinder speed can be washed and graded in a short time which is the reason for higher through output capacity. Therefore, on average, this machine can wash and grade above 242.17 kg carrot tuber per hour which is better when compared to (Ambrose and Annamalai, 2013) and the traditional method that needs above one hour to wash and grade 100kg carrot roots.

Generally, as discussed above the average minimum required time (2.22 min), the maximum washing efficiency (98.7%), the maximum grading efficiency (92.23), the maximum throughput put capacity (242.17 kg h⁻¹), and the optimum percentage of damage (1.21%) was recorded at 2.93 m s⁻¹ and 10 kg feeding load which is recommended as the better working condition of the machine.

4 Conclusion

A carrot washing and grading machine was designed, constructed, and evaluated. It consists mainly of four parts: the pedal assembly (power transmission unit), the reciprocating pump assembly, washing and grading cylinder, and supporting frame. The machine was evaluated using the ‘Nantay’ variety at different cylinder speeds (1.47, 2.201, and 2.93 m s⁻¹) with two-level of feeding loads (10 kg and 15 kg). The performance

evaluation revealed the following:

The average minimum time required for washing was 2.22 minutes. it tended to increase with the increase in drum speed and decrease with the feeding load.

The overall mean washing and grading efficiencies were 98.70% and 92.23% respectively. Both of them tend to increase with the increase in drum speed and decrease with the increase in feeding load.

Lowering both cylinder speed and feed load tends to reduce the percentage of damage while low feed load and high cylinder speed tend to minimize the time required to complete activities.

Both washing and grading efficiency of the carrots a washing and grading machine is significantly affected by the independent variables, namely: cylinder speed and feeding load.

The throughput capacity increases as speed increases. The machine has an overall mean throughput capacity of 242.17 kg h⁻¹. The unit cost of the washing and grading machine was \$313.18, which is cheap and affordable for an average Ethiopian farmers.

The carrots have low sphericity (0.30%), which causes them to always roll when they are on a particular orientation or axis, leading to some amount of incorrectly graded carrot roots being registered. Therefore, for better

washing efficiency, the grading unit should be modified to a vibration mechanism by separating it from the washing unit in a layer of the machine frame.

Acknowledgments

Appreciation is extended to Haramaya University Department of Agricultural Engineering and Adama Science and Technology University Department of Mechanical Engineering for their valuable support.

References

- Adegbite, S. A., S. K. Adeyemi, A. O. Komolafe, M. O. Salami, C. F. Nwaeche, and A. A. Ogunbiyi. 2019. Design and development of fruit washer. *Journal of Scientific Research and Reports*, 21(6): 1–11.
- Adekanye, T. A., A. B. Osakpamwan, and I. E. Osaivbie. 2016. Evaluation of a soybean threshing machine for small scale farmers. *CIGR Journal*, 18(2): 426–434.
- Adzimah, S. K., and H. E. Agbovi. 2015. Foot-operated device for controlling the flow of water into plumbing fixtures. *Innovative Systems Design and Engineering*, 6(5): 18–36.
- Ahmad, T., M. Cawood, Q. Iqbal, A. Ariño, A. Batool, R. M. Sabir Tariq, M. Azam, and S. Akhtar. 2019. Phytochemicals in *Daucus carota* and their health benefits. *Foods*, 8(9): 424.
- Ajay, Jadoun, R. S., Choudhary, & Choudhary, S. K. 2014. Design & fabrication of manually driven pedal powered washing machine. *Innoovative System Design and Engineering*, 5(6), 56–67.
- Alam, S., P. Chavan, and R. Sharma. 2018. Post harvest value chain of carrot-A Review. *Agricultural Engineering Today*, 42(4): 1–11.
- Ambrose, D. C. P. and S. J. K. Annamalai. 2013. Development of a manually operated root crop washer. *African Journal of Agricultural Research*, 8(24): 3097–3101.
- Amin, M. N., and M. A. Hossain. 2021. Development and evaluation of a mechanical carrot washing machine. *CIGR Journal*, 23(3): 111-120.
- Anjali, M., and M. S. R. Ikhar. 2018. Design and development of rotary type vegetable cleaner. *International Journal for Scientific Research & Development*, 6(03): 878–880.
- Antony, S., A. Arjun, T. K. Shinos, and P. Anoop. 2016. Design and analysis of a connecting rod. *International Journal of Engineering Research & Technology*, 5(10): 188–192.
- Ashiedu, F. I., T. C. Nwaoha, and C. O. Izelu. 2016. Design and development of a manual pump for agrarian communities. *International Journal of Current Research*, 8(3): 27378–27382.
- Bashar, Z. U., A. Wayayok, A. M. S. Mohd. 2014. Determination of some physical properties of common malaysian rice MR219 seeds. *Austrian Journal of Crop Science*, 8(3): 332–337.
- Bayram, M., Ö. Şahin, and O. Arslan. 2018. Sphericity measurement techniques for solid materials. In *International Gap Agriculture & Livestock Congress*, 992-994. Sanliurfa, Turkey, 25-27 April.
- Bender, I., L. Edesi, I. Hiiesalu, A. Ingver, T. Kaart, H. Kaldmäe, T. Talve, I. Tamm, and A. Luik. 2020. Organic carrot (*Daucus carota* L.) production has an advantage over conventional in quantity as well as in quality. *Agronomy*, 10(9): 1420.
- Bharath Kumar, K., Bibin George Thomas, Paul James Thadhani, and A. Pandiyan. 2015. Design and analysis of connecting rod using composite materials.” *International Journal of Applied Engineering Research* 10 (65): 236–241.
- Bhatawadekar, G., B. Salman, N. Chiplunkar, S. Devrukhakar, and S. Akashdeep. 2015. Design and fabrication of pedal powered washing machine. *International Journal of Engineering Research and General Science*, 3(1): 1307–1311.
- Bhattarai, D. R., G. D. Subedi, I. P. Gautam, and S. Chauhan. 2017. Postharvest supply chain study of carrot in Nepal. *International Journal of Horticulture*, 7(26): 239-245.
- Boukouvalas, C. J., G. I. Bisharat, and M. K. Krokida. 2010. Structural properties of vegetables during air drying. *International Journal of Food Properties*, 13(6): 1393-1404.
- CSA, R. "The federal democratic republic of Ethiopia central statistical agency report on area and production of major Crops. Stat." Bull (2016).
- Dereje, A. A. 2019. Design, manufacturing and performance evaluation of potato grading machine (unpublished). M.S. thesis, Haramaya University.
- El-Rahman, Abd, and Magda Mosa. 2011. Development and evaluation of a simple grading machine for okra pods. *Journal of Soil Sciences and Agricultural Engineering* 10 (4): 227–232.
- FAO. 2018. Crops and Livestock Products. Available at: <https://www.fao.org/faostat/en/#compare>. Accessed February 20, 2022.
- Gautam, A., R. Khurana, G. S. Manes, and A. K. Dixit. 2016. Studies on engineering properties of pelleted carrot (*Daucus carota* L.) seeds. *International Journal of BioResource and Stress Management*, 7(5): 1044–1048.

- Goud, P. Karthik Kumar, and T. Sumalatha. 2018. Design and Analysis of Automatic Double Acting Multi Cylinder Pneumatic Reciprocating Pump. *International Journal of Innovative Technologies* 06 (02): 491–98.
- Gujar, R. A., and S. V. Bhaskar. 2013. Shaft design under fatigue loading by using modified goodman method. *International Journal of Engineering Research and Applications*, 3(4): 1061–1066.
- Guru, D. K., S. P. Singh, S. Tiwari, S. Pal, and S. K. Shukla. 2019. Design and working of pedal operated flour mill. *International Journal of Trend in Scientific Research and Development*, 3(3): 1279–1280.
- Hakizimana, E., P. Masengesho, O. Cyusa, and M. Niyigena. 2020. Design and analysis of a pedal operated washing and drying machine. *Journal of Applied Mechanical Engineering*, 9(4): 338.
- Jahanbakhshi, A., Y. Abbaspour-Gilandeh, and T. M. Gundoshmian. 2018. Determination of physical and mechanical properties of carrot in order to reduce waste during harvesting and post-harvesting. *Food Science and Nutrition*, 6(7): 1898–1903.
- Khurmi, R. S., and J. K. Gupta. 2005. *A Textbook of Machine Design*. 14th ed. Ram Nagar, New Delhi-110: Eurasia publishing house (PVT.) LTD.
- Krishnamurthy, M., K. K. Rakshith, R. Harshaa, and N. Rakesh. 2017. Pedal operated washing machine. *International Journal of Latest Engineering Research and Applications*, 02(05): 60–66.
- Moos, J. A., D. D. Steele, and D. C. Kirkpatrick. 2002. Small-scale mechanical carrot washer for research sample preparation. *Applied Engineering in Agriculture*, 18(2): 235–241.
- Mukkawar, V. V., A. P. Kadam, A. Ingole, and M. Chopade. 2015. Design, analysis and optimization of connecting rod using ANSYS. *International Journal of Advances in Mechanical and Civil Engineering*, 2(2): 38–41.
- Mushiri, T., T. J. Mugova, and C. Mbohwa. 2017. Design and fabrication of a pedal powered washing machine. In *Proc. of the International Conference on Industrial Engineering and Operations Management*, 355–366. Bogota, Colombia, October 25–26.
- Nitturkar, H. D., S. M. Kalshetti, and A. R. Nadaf. 2020. Design and analysis of connecting rod using different materials. *International Research Journal of Engineering and Technology*, 7(3): 1011–1017.
- Patil, S., M. Deore, B. Swami, and O. Bhabad. 2021. Design calculation of agricultural reaper. *International Research Journal of Engineering and Technology*, 8(5): 739–748.
- Seweh, E. A., J. O. Darko, A. Addo, P. A. Asagadunga, and S. Achibase. 2016. Design, construction and evaluation of an evaporative cooler for sweet potatoes storage in the north China. *CIGR Journal*, 18(2): 435–448.
- Shankar, R., A. Suhane, and M. Vishwakarma. 2016. Overhauling of two stage reciprocating air compressor of a conventional locomotive-a case study. *International Research Journal of Engineering and Technology*, 3(4): 653–664.
- Sharma, D. N., and S. Mukesh. Farm machinery design. Principles and Problems. JAIN Brothers, Neew Delhi (2010).
- Siddique, G., A. Aleem, G. Hussain, and H. A. Raza. 2017. Development and performance evaluation of carrot washer. *Journal Global Innovation Agriculture Social Science*, 5(1): 28–31.
- Soyoye, B. O., O. C. Ademosun, and L. A. S. Agbetoye. 2018. Determination of some physical and mechanical properties of soybean and maize in relation to planter design. *CIGR Journal*, 20(1): 81–89.
- Surbhi, S., R. C. Verma, R. Deepak, H. K. Jain, and K. K. Yadav. 2018. A review : Food, chemical composition and utilization of carrot (*Daucus carota* L.) pomace. *International Journal of Chemical Studies*, 6(3): 2921–2926.
- Tabor, G., and M. Yesuf. 2012. Mapping the current knowledge of carrot cultivation in Ethiopia. Denmark: Carrot Aid,.
- Teferra, T. F. 2019. Engineering properties of food materials. In *Handbook of farm, dairy and food machinery engineering* (pp. 45–89). Academic Press.
- Thorat, S. D., and A. B. K. Patil. 2015. Study of performance analysis of reciprocating pumps using CFD. *Ird-India Advance Physics Letter*, 4(1): 40–46.1
- Umami, K. C., and I. E. Markson. 2020. Development and performance evaluation of a manually operated onions grading machine. *Journal of Agriculture and Food Research*, 2: 100070.
- Vegi, L. K., and V. G. Vegi. 2013. Design and analysis of connecting rod using forged steel. *International Journal of Scientific & Engineering Research*, 4(6): 2081–2090.
- Yadav, P. 2020. A Review on different types of carrot and its chemical compositions. *IOSR Journal of Pharmacy*, 10(5): 32–39.